Indian Journal of Pure & Applied Physics
Vol. 58, April 2020, pp. 241-245

^{58}Ni(n,p)^{58}Co and ^{58}Ni(n,2n)^{57}Ni reactions at the neutron energy of 14.54 MeV with covariance analysis

Imran Pasha[a*], B Rudraswamy[a], Y S Sheela[b], S V Suryanarayana[c], E Radha[d] & Rebecca Pachuau[e]

[a]Department of Physics, Bangalore University, Bengaluru 560 056, India
[b]Department of Statistics, Manipal Academy of Higher Education, Manipal 576 104, India
[c]Nuclear Physics Division, Bhabha Atomic Research Center, Mumbai 400 854, India
[d]RPD, ROMG, IGCAR, Kalpakkam, Tamilnadu 603 102, India
[e]Department of Nuclear and Atomic Physics, Tata Institute of Fundamental Research, Homi Bhabha Road, Colaba, Mumbai 400 005, India

Received 17 February 2020

The ^{58}Ni(n,p)^{58}Co and ^{58}Ni(n,2n)^{57}Ni reactions cross sections have been estimated relative to ^{197}Au(n,2n)^{196}Au monitor reaction at the incident neutron energy of 14.54±0.0024 MeV from the D-T fusion nuclear reaction using Purnima neutron generator carried through methods of activation and off-line γ-ray spectrometry. The uncertainty propagation and correlation for measured cross sections have been estimated using covariance analysis through considering the partial uncertainties in different attributes. The present measured reaction cross sections data have been analyzed by comparing with the literature data, with various libraries of evaluated data, like ENDF/B-VIII.0, JEFF-3.3, JENDL/AD-2017, ROSFOND-2010 and TALYS-1.9 theoretical calculations.

Keywords: ^{58}Ni(n,p)^{58}Co and ^{58}Ni(n,2n)^{57}Ni reaction, D-T fusion reaction, γ-ray spectrometry, Covariance, TALYS-1.9

1 Introduction

The database of neutron induced reaction cross sections in the neutron energy range 12-20 MeV has very essential applications in nuclear fusion and fission reactors, nuclear technology, validation of theoretical nuclear models, testing nuclear reaction model, astrophysics, medical and industries[1]. Nickel is a silvery-white lustrous metal, hard and ductile. It is an decisive component of many types of materials such as steel, cladding alloy link zircaloy-2 in fission and fusion reactor technologies [2]. The reaction cross sections data of nickel could give useful information on hydrogen gas production, for estimation of the radiation damage to the reactor structural and cladding materials[3]. On the basis of literature review, cross sections data are available for ^{58}Ni(n,p)^{58}Co [2-7] and ^{58}Ni(n,2n)^{57}Ni [2,4,5,7-12] reactions for the neutron energy 12-20 MeV. Thus there are a few experimental cross section data available for the ^{58}Ni(n,p)^{58}Co and ^{58}Ni(n,2n)^{51}Ni reactions for the neutron energy at 14.54±0.0024 MeV. Many cross section data do not have uncertainty information due to errors in attributes such as half life, gamma abundances, efficiency, etc., and detectors, used. The error free cross sections data for ^{58}Ni(n,p)^{58}Co and ^{58}Ni(n,2n)^{57}Ni reactions are still not met the requirement and hence need improvement. In view of above facts, it is important to study the neutron induced cross sections for the ^{58}Ni(n,p)^{58}Co and ^{58}Ni(n,2n)^{51}Ni reactions for the neutron energy 12-20 MeV.

Considering above evidences, the ^{58}Ni(n,p)^{58}Co and ^{58}Ni(n,2n)^{57}Ni reactions cross sections have been estimated relative to ^{197}Au(n,2n)^{196}Au monitor reaction at the incident neutron energy of 14.54±0.0024 MeV. We followed the methods of activation and off-line γ-ray spectrometry. The ^{58}Ni(n,p)^{58}Co and ^{58}Ni(n,2n)^{57}Ni reactions cross sections, plotted as a function of neutron energy within range of 12-20 MeV. The plotted data are analyzed by comparing with the literature data, with various libraries of evaluated data and as well as with default parameters of TALYS-1.9 [13].

2 Experimental Details

The experiment was carry out by using Purnima neutron generator based on the Cockcroft-Walton generator at Bhabha Atomic Research Center (BARC), Mumbai. The deuterium gas supplied to an RF ion source through which D^+ ions are generated

*Corresponding author (E-mail: imranp905@gmail.com)

and collected, focused. The focused D^+ ions were accelerated and incident on a titanium–tritium (TiT) target. The details of Purnima neutron generator are given else where[14].

In the current experiment the D^+ ion were accelerated to 180 kV which was impinged on TiT target. The ^{nat}Ni and ^{197}Au foils procured from Alfa Aeaser, USA. The ^{nat}Ni and ^{197}Au foils of weights 130 and 126 mg, respectively, were taken and wrapped in a 0.011 mm thick Al foil to protect the targets from the radioactive impurities within the targets during irradiation. A stack of Ni-Au samples was mounted at zero degree angle relative to the beam direction. The stack foils of Ni-Au was irradiated for 2 h with the neutron beam produced from the ^{3}H(d,n)^{4}He reaction. After the irradiation, samples were taken out and cooled for 0.2-1.2 h. The γ-emitting samples of Ni-Au along with Al wrapper were mounted on separate Perspex plates and then taken for γ-ray spectrometry. The γ-ray counting of the irradiated foils were perform using a Baltic HPGe detector having 30% relative efficiency and coupled to a PC-based 4k multichannel analyzer. The γ-ray acquisition was done using LAMPS (Linux Advance Multi Parameter System) software. The resolution of the HPGe detector has a FWHM of 1.8 keV at 1.33 MeV γ-ray for ^{60}Co. The ^{152}Eu calibration source used to perform efficiency calibration of the HPGe detector keeping the source at a distance of 1 cm from the detector end cap to decrease summing effect.

3 Calculations and Data Analysis

3.1 Efficiency calibration of HPGe detector with uncertainty

The ^{152}Eu calibration source used to perform efficiency calibration of the HPGe detector. The source activity (A_0) was 5036.89±70.97 Bq as on 1 October 1999. The efficiency of HPGe detector was estimated by the following expression:

$$\varepsilon(E_\gamma) = \frac{CK_C}{I_\gamma A_0 e^{-0.693t/T_{1/2}}} \quad \ldots (1)$$

where E_γ is γ-ray energy, $\varepsilon(E_\gamma)$ is efficiency, C is detected γ-ray counts for 1293 s from the ^{152}Eu γ-ray spectrum, $T_{1/2}$ is half-life (13.517±0.014 y), t is elapsed time between date of manufacture of calibration source and detector calibration (19.62 y). The half-life, γ-ray abundance (I_γ) at each of the eight γ-ray energies of ^{152}Eu were retrieved from Nu Dat 2.7[15,16]. The coincidence summing effect K_C was determined using EFFTRAN code[17]. The counts and auxiliary data presented in Table 1 are then used in Eq. (1) to obtain efficiency $\varepsilon(E_\gamma)$ at each of the eight identified γ-ray energy the data of the same are summarized in column 5 of Table 1.

The methodology for obtaining the covariance matrix (V_ε) is as given in earlier studies[18,19]. The known γ-ray energies of ^{152}Eu source is different from characteristic γ-ray energies of the reaction products ^{58}Co, ^{57}Ni and ^{196}Au. Therefore to determine the efficiencies of detector corresponding to the γ-rays of ^{58}Co, ^{57}Ni and ^{196}Au nuclides, we considered following linear parametric function:

$$In(\varepsilon_i) = \sum_{k=1}^{m} p_k (\ln [E_i])^{k-1} \; 1 \le i \le 11, 1 \le k \le m \quad \ldots (2)$$

We estimated, the goodness of fit value was observed for n=4, with $\frac{\chi^2}{11-4} = 1.444 \approx 1$. We consider the following linear parametric model as the best model, which is presented below:

$$ln\varepsilon = -3.652 - 0.873lnE + 0.155(lnE)^2 + 0.097(lnE)^3 \quad \ldots (3)$$

Equation (3) was used to estimate the efficiencies corresponding to γ-rays emitted from the reaction products ^{58}Co, ^{57}Ni and ^{196}Au. Table 2 presents the estimated efficiencies of detector corresponding the reaction products with correlations. The estimated

Table 1 — Efficiency calibration of HPGe detector using ^{152}Eu.

E_γ (MeV)	I_γ (%)	C	K_c	$\varepsilon(E_\gamma)$
0.121	28.53±0.16	71567±1637	1.24	1.30E-01
0.244	7.55±0.04	12648±240	1.35	9.48E-02
0.344	26.59±0.20	37870±426	1.15	6.87E-02
0.411	2.24±0.013	2225±72	1.41	5.86E-02
0.688	0.86±0.006	725±59	1.09	3.86E-02
0.778	12.93±0.08	8240±184	1.23	3.29E-02
0.867	4.23±0.03	2045±77	1.42	2.89E-02
0.964	14.51±0.07	8114±149	1.16	2.72E-02
1.112	13.67±0.08	7007±148	1.08	2.34E-02
1.299	1.63±0.011	592±51	1.41	2.14E-02
1.408	20.87±0.09	8662±156	1.12	1.95E-02

Table 2 — Interpolated detector efficiencies and correlation matrix

Nuclide	γ-ray Energy (keV)	ε_c	$V_{\varepsilon c}$ (x10^{-07})			$C_{\varepsilon c}$		
^{58}Co	811	0.031	3.594			1		
^{57}Ni	1378	0.015	1.147	1.704		0.463	1	
^{196}Au	356	0.059	5.018	2.419	14.087	0.705	0.494	1

efficiencies presented in Table 2 are required for further cross sections calculation. The procedure we used in estimating the efficiencies corresponding to the characteristic γ-rays of reaction products with covariance analysis was given in earlier studies[20,21].

3.2 Neutron energy calculation

Geant 4 allows the simulation of the interaction of radiation with matter. It is used in applications such as high energy physics, space science, astrophysics, and medical physics, in detector modeling visualization as well as in reverse Monte Carlo simulation[22]. The neutron energy spectrum at 180±0.1 keV deuteron energy is simulated using Geant4, in a convolution with deuteron energy loss and differential cross section. The head geometry and samples is simulated in the geometry class[22]. Deuteron beam diameter, shape, energy and energy spread etc are also incorporated for the final energy production[23]. Similarly the effect of steel flank, angular coverage of sample are also taken into account. The ENDF/B-VI[24] differential cross section was used for calculation. A sensitive detector function is defined on the sample to read the energy of neutrons hitting on the sample. The neutron energy data projected into a histogram and normalized with the total number of events. The neutron energy spread is calculated from the standard deviation of fitted gaussian as (FWHM/centroid). The neutron energy is found to be 14.54±0.002 MeV.

3.3 ^{58}Ni(n,p)^{58}Co and ^{58}Ni(n,2n)^{57}Ni reactions cross sections with covariance analysis

To estimate the ^{58}Ni(n,p)^{58}Co and ^{58}Ni(n,2n)^{57}Ni reactions cross sections at the neutron energy of 14.54±0.0024 MeV, used the following expression:

$$\sigma_S = \sigma_M \frac{\frac{C_S \lambda_S W t_M a_M A_{VS} I_{\gamma M} \varepsilon(E_\gamma)_M \left(1-e^{-\lambda t_{iM}}\right)}{\left(e^{-\lambda t_{dM}}\right)\left(1-e^{-\lambda t_{cM}}\right)}}{\frac{C_M \lambda_M W t_S a_S A_{VM} I_{\gamma S} \varepsilon(E_\gamma)_S \left(1-e^{-\lambda t_{iS}}\right)}{\left(e^{-\lambda t_{dS}}\right)\left(1-e^{-\lambda t_{cS}}\right)}} \prod_k \frac{(C_k)_m}{(C_k)_S} \quad \ldots (4)$$

The subscripts S and M appearing in Eq. (4) represents the sample and monitor, $\sigma_s(E_n)$ and $\sigma_M(E_n)$ represent the reaction cross sections at the neutron energy E_n respectively, C_S and C_M are the detected γ-ray peak counts of ^{58}Co, ^{57}Ni respectively, λ_S and λ_M represent decay constants, Wt_S and Wt_M represent weights, a_S and a_M represent isotopic abundances, A_{VS} and A_{VM} represent average atomic masses, $I_{\gamma S}$ and $I_{\gamma M}$ represent the γ-ray abundances, $\varepsilon(E_\gamma)_S$ and $\varepsilon(E_\gamma)_M$ represent efficiencies of ^{58}Co, ^{57}Ni radionuclide's respectively, t_i, t_d and t_C represent irradiation, decay and counting time, $(C_k)_S$ and $(C_k)_M$ represent the correction factors, where k represent the dead time detector and γ-ray self-attenuation factor (Γ_{attn}). We estimated self-attenuation factor (Γ_{attn}) and μ mass attenuation coefficient retrieve from XMuDat ver. 1.0.1 for the irradiated foils using procedure given in earlier studies[25,26]. The monitor cross section of ^{197}Au(n,2n)^{196}Au reaction at the neuron energy 14.54±0.0024 MeV was obtained by considering the cross section values at the nearest energy points, which is obtained as 2.1236±0.02049 barns [27].

The basic nuclear spectroscopic data with uncertainties are summarized in Table 3, which are retrieved from NuDat 2.7 database[16]. The terms that are observed with error are σ_M, C_S, C_M, λ_S, λ_M, Wt_S, Wt_M, a_S, A_{VS}, A_{VM}, $I_{\gamma S}$, $I_{\gamma M}$, $\varepsilon(E_\gamma)_S$, $\varepsilon(E_\gamma)_M$, $(\Gamma_{attn})_S$, $(\Gamma_{attn})_M$ and other terms such as a_M, t_i, t_d, t_C appearing in Eq. (4) are observed without error.

The i[th], j[th] entry of covariance matrix $V_{\sigma S}$ corresponding reaction products estimated as follows:

$$(V_{\sigma S})_{ij} = \sum_{kl} [\![(e]\!]_k)_i (s_{kl})_{ij} [\![(e]\!]_l)_j \,, 1 \le i,j \le 3, 1 \le k,l \le 16 \quad \ldots (5)$$

where $(s_{kl})_{ij}$ is the correlation between the k^{th} attribute in the i[th] experiment and l^{th} attribute in the j[th] experiment and $(e_k)_i = \frac{\partial \sigma_{Si}}{\partial (x_k)_i} \Delta(x_k)_i$, $(e_l)_j = \frac{\partial \sigma_{Sj}}{\partial (x_l)_j} \Delta(x_l)_j$ is partial uncertainties in σ_{Si}, σ_{Sj} due to the k[th], l^{th} attributes respectively. The fractional uncertainties from different attributes present in the measured reactions of ^{58}Ni(n,p)^{58}Co and ^{58}Ni(n,2n)^{57}Ni

Table 3 — Nuclear spectroscopic data of reaction product required for the estimation of $\sigma_s(E_n)$.

Nuclear reaction	Threshold energy (MeV)	Half-life	γ-ray energy (keV)	γ-ray Intensity (%)	Decay mode (%)
^{58}Ni(n,p) ^{58}Co	0.0	70.86±0.06 d	810.7	99.45±0.01	ε (100)
^{58}Ni(n,2n) ^{57}Ni	12.428	35.60±0.06 h	1377.6	81.70±0.24	ε (100)
^{197}Au(n,2n)^{196}Au	8.114	6.1669±0.0006 d	355.7	87±3	ε (93) + β^-(7)

cross section with respect to ^{197}Au(n,2n)^{196}Au monitor reaction are listed in Table 4. The correlations obtained between three observations are listed in the last column of Table 4. Detailed descriptions on micro correlation matrices, the readers are refer [28,29]. The results of the estimated reactions ^{58}Ni(n,p)^{58}Co and ^{58}Ni(n,2n)^{57}Ni cross section at the neutron energy of 14.54±0.0024 MeV with its uncertainties and correlations matrix are presented in Table 5.

4 Discussion

The ^{58}Ni(n,p)^{58}Co and ^{58}Ni(n,2n)^{57}Ni reactions cross sections have been estimated relative to ^{197}Au(n,2n)^{196}Au monitor reaction at the incident neutron energy of 14.54±0.0024 MeV through methods of activation and off-line γ-ray spectrometry. The cross sections of two different reactions were determined using ratio method. We determined uncertainties considering various attributes in the data using the covariance analysis and correlations between them. The computer code TALYS-1.9 was used for the analysis and prediction of nuclear reaction cross sections values based on the nuclear models. In the present work, the cross sections for the ^{58}Ni(n,p)^{58}Co and ^{58}Ni(n,2n)^{57}Ni reactions within the neutron energy range of 12-20 MeV were theoretically calculated using the TALYS-1.9 code with default parameters.

The cross sections for the ^{58}Ni(n,p)^{58}Co and ^{58}Ni(n,2n)^{57}Ni reactions from the present work, evaluated data, like ENDF/B-VIII.0 [30], JEFF-3.3 [31], JENDL/AD-2017 [32] and ROSFOND-2010 [33] libraries, literature data [2-12] available in EXFOR [34], as well as the TALYS-1.9 [13] within 12-20 MeV are seen in Figs 1 and 2. It can be seen from Figs 1 and 2, that the present data at the neutron energy of 14.54±0.0024 MeV

Table 4 — Fractional uncertainties (%) and correlations of measured reactions

Attributes	Nuclide ^{58}Co	Nuclide ^{57}Ni	Correlation
σ_M	0.9651	0.9651	fully correlated
C_S	7.3324	5.7354	uncorrelated
C_M	0.9293	0.9293	fully correlated
λ_S	1.412E-03	1.377E-02	uncorrelated
λ_M	0.6542	0.6542	fully correlated
Wt_S	2.213E-02	2.213E-02	fully correlated
Wt_M	2.283E-02	2.283E-02	fully correlated
a_S	1.322E-02	1.322E-02	fully correlated
A_{VS}	6.904E-06	6.904E-06	fully correlated
A_{VM}	3.046E-07	3.046E-07	fully correlated
$I_{\gamma S}$	1.005E-02	2.937E-02	uncorrelated
$I_{\gamma M}$	0.3448	0.3448	fully correlated
$\varepsilon(E_\gamma)_S$	1.9128	2.6865	uncorrelated
$\varepsilon(E_\gamma)_M$	1.9883	1.9883	fully correlated
$(\Gamma_{attn})_S$	0.3037	0.2317	uncorrelated
$(\Gamma_{attn})_M$	0.6542	0.6542	fully correlated

Table 5 — The experimentally determined reaction cross sections relative to the ^{197}Au(n,2n)^{196}Aumonitor reaction with its uncertainty and correlation matrix

Reaction	Cross section (barns)	Correlation	
^{58}Ni(n,p)^{58}Co	0.3469±0.02777	1	
^{58}Ni(n,2n)^{57}Ni	0.0247±0.00168	0.1176	1

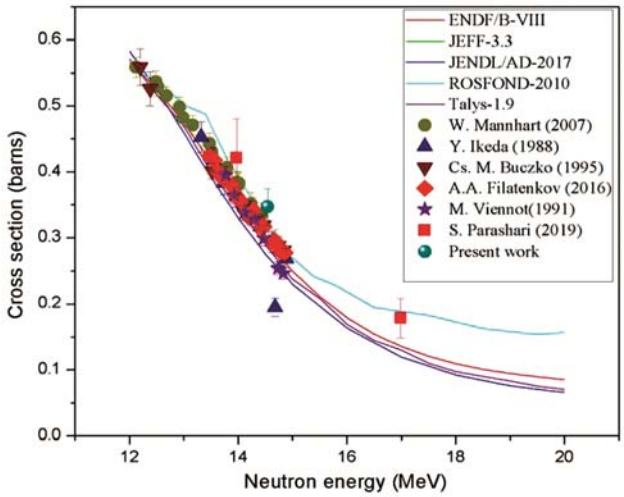

Fig. 1 — Plot of ^{58}Ni(n,p)^{58}Co reaction cross section from the present work with the literature data, evaluated data of ENDF/B-VIII.0, JEFF-3.3, JENDL/AD-2017 and ROSFOND-2010 libraries as well as with TALYS-1.9 as a function of neutron energy.

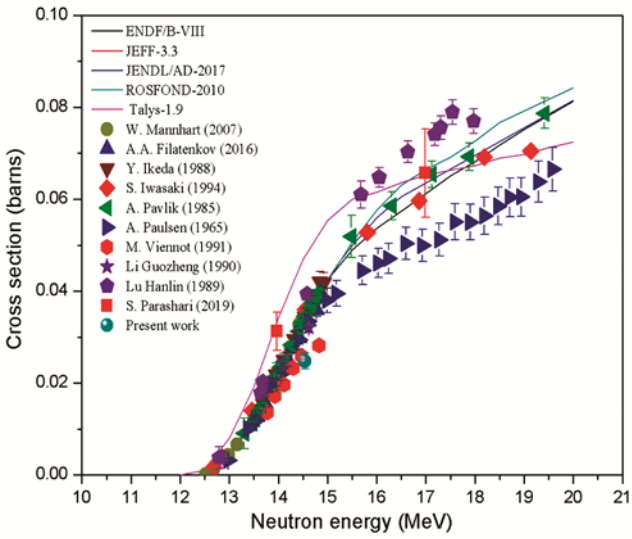

Fig. 2 — Plot of ^{58}Ni(n,2n)^{57}Ni reaction cross section from the present work with the literature data, evaluated data of ENDF/B-VIII.0, JEFF-3.3, JENDL/AD-2017 and ROSFOND-2010 libraries as well as with TALYS-1.9 as a function of neutron energy.

is in well agreement with the theoretical value from TALYS-1.9 and with ENDF/B-VIII.0, JEFF-3.3, JENDL/AD-2017 and ROSFOND-2010 libraries as well as with the literature data.

5 Conclusions

The ^{58}Ni(n,p)^{58}Co and ^{58}Ni(n,2n)^{57}Ni reactions cross sections have been measured relative to the ^{197}Au(n,2n)^{196}Au monitor reaction at the neutron energy of 14.54±0.0024 MeV by using the methods of activation and off-line γ-ray spectrometry. The ^{152}Eu calibration source used to perform efficiency calibration of the HPGe detector with covariance analysis. We executed covariance analysis method to estimate uncertainties of the cross sections data, which was carried out using error analysis and micro-correlation. The uncertainty in the measured cross sections were found within the range of 6-8%. The ^{58}Ni(n,p)^{58}Co and ^{58}Ni(n,2n)^{57}Ni reactions cross sections from the present studies have been compared and found to be in well agreement with the evaluated data of various libraries, literature data and TALYS-1.9.

Acknowledgement

The work was financially supported by Department of Atomic Energy & Board of Research in Nuclear Sciences (DAE-BRNS) through major research project (Sanction No. 36(6)/14/ 92/2014-BRNS/2727). The author (IP) is thankful to Directorate of Minorities, Govt. of Karnataka and would like to thank the staff of Purnima neutron generator for their kind support to perform experiment.

References

1 Belgaid M, Siad M & Allab M, *J Radioanal Nucl Chem Lett*, 166 (1992) 493.
2 Parashari S, Mukherjee S, Naik H, Suryanarayana S V, Makwana R, Nayak B K & Singh N L, *Eur Phys J*, A55 (2019) 51.
3 Buczko C M, Csikai J, Sudar S, Grallert A, Jonah S A, Jimba B W, Chimoye T & Wagner M, *Phys Rev C*, 4 (1995) 52.
4 Manhart W & Schmidt D, *Neutronenphysik Reports*, 53 (2007).
5 Ikeda Y, Konno C, Oishi K, Nakamura T, Miyade H, Kawade K, Yamamoto H & Katoh T, *JAERI Reports*, 1312 (1988).
6 Filatenkov A A, INDC (CCP)-0460 Rev (2016).
7 Viennot M, Berrada M, Paic G & Joly S, *Nucl Sci Eng*, 108 (1991) 289.
8 Iwasaki S, Matsuyama S, Ohkubo T, Fukuda H, Sakuma M & Kitamura M, *Conf Nucl Data Sci Tech*, 1 (1994) 305.
9 Pavlik A, Winkler G, Uhl M, Paulsen A & Liskien H, *Nucl Sci Eng*, 90 (1985) 186.
10 Paulsen V A & Liskien H, *J Nukleonik*, 7 (1965) 117.
11 Guozheng L & Jiang J, *High Energy Physics Nucl Phys Chinese Edn*, 14 (1990) 1023.
12 Hanlin L, Jianzhou H, Fan P, Yunfeng C & Zhao W, *Chinese Report INDC*, 16 (1989).
13 Koning A J, Hilaire S & Goriely S, TALYS-1.9, (2017). http://www.talys.eu/download-talys/
14 Sinha A, Roy T, Yogesh K, Nirmal R, Shukla M, Patel T, Bajpai S, Sarkar P S & Bishnoi S, *Nucl Instrum Methods Phys Res B*, 350 (2015) 66.
15 Martin M J, *Nucl Data Sheets*, 114 (2013) 1497.
16 NuDat 2.7 (2016). http://www.nndc.bnl.gov/nudat2
17 Tim V, *Nucl Instrum Methods Phys Res A*, 550 (2005) 603.
18 Sheela S Y, Naik H, Manjunatha K M, Ganesan S & Suryanarayana S V, Internal report, No. Mu/Stastics/DAE-BRNS/2017, DOI:10.13140/RG.2.2.26729.49764 (2017).
19 Geraldo L P & Smith D L, *Nucl Instrum Methods Phys Res A*, 290 (1990) 499.
20 Pasha I, Rudraswamy B, Radha E & Sathiamoorthy V, *Radiat Prot Environ*, 41 (2018) 110.
21 Geraldo L P & Smith D L, *Inst de Pesquisas Energeticase Nuleares*, 243 (1989) 1.
22 Agostinelli S, Allison J, Amako K et al., *Nucl Instru Meth Phys Res A*, 506 (2003) 250.
23 Patel T & Sinha A, *BARC Newsletter*, 146 (2013).
24 Carlson A D, Poenitz W P, Hale G M, Peelle R W, Doddler D C, Fu C Y & Mannhart W, *National Institute of Standards and Technology Internal Report*, 5177 (1993).
25 Millsap D W & Landsberger S, *Appl Radiat Isot*, 97 (2015) 21.
26 Nowotny R, XMu Dat (1998). http://www-nds.iaea.org/publications/iaea-nds.
27 Capote R, Zolotarev K I, Pronyaev V G & Trkov A, (2012) IRDF-2002. http://www-nds.iaea.org/IRDFF/
28 Yerraguntla S S, Naik H, Karantha M P, Ganesan S, Suryanarayana S V & Badwar S, *J Radio Anal Nucl Chem*, 314 (2017) 457.
29 Pasha I, Basavanna R, Suryanarayana S V, Sheela S S, Meghna K, Naik H, Prasad M K, Danu L S, Saroj B, Patel T & Rajeev K, *J Radioanal Nucl Chem*, 320 (2019) 561.
30 Herman M & Trkov A, *Nuclear Data Sheets*, 148 (2018) 214.
31 Koning A J, Bauge E, Dean C J, Dupont E, Fisher U, Forrest R A, Jacqmin R, Leeb H, Kellet M A, Mills R W, Nordborg C, Pescarine M, Rungma Y & Rullhusen P, *Kor Phys Soc*, 59 (2011) 1057.
32 Shibata K, Iwamot N, Kunieda S, Minato F & Iwamoto O, JAEA, (2016) 47.
33 Zabrodskaya S V, Ignatyuk A V & Koscheev V N, *Nuclear constants*, ROSFOND-2010 (2007) 1.
34 IAEA-EXFOR Database available at http://www-nds.iaea.org/exfor.